

Electronic Supplementary Material

Inversion symmetry broken 2D SnP₂S₆ with strong nonlinear optical response

Yue Zhang¹, Fakun Wang¹, Xin Feng¹, Zongdong Sun¹, Jianwei Su¹, Mei Zhao¹, Shuzhe Wang¹, Xiaozong Hu² (✉), and Tianyou Zhai¹ (✉)

¹ State Key Laboratory of Materials Processing and Die & Mould Technology, and School of Materials Science and Engineering, Huazhong University of Science and Technology, Wuhan 430074, China

² Henan Key Laboratory of Crystalline Molecular Functional Materials, Henan International Joint Laboratory of Tumor Theranostical Cluster Materials, Green Catalysis Center, and College of Chemistry, Zhengzhou University, Zhengzhou 450001, China

Supporting information to <https://doi.org/10.1007/s12274-021-3806-0>

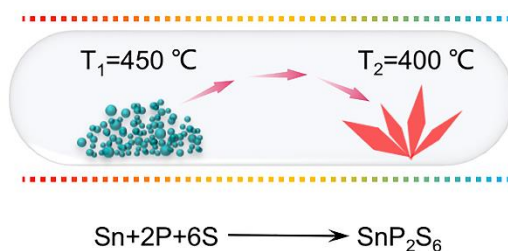


Figure S1 Schematic illustration of the CVT synthesis SnP₂S₆ single crystals.

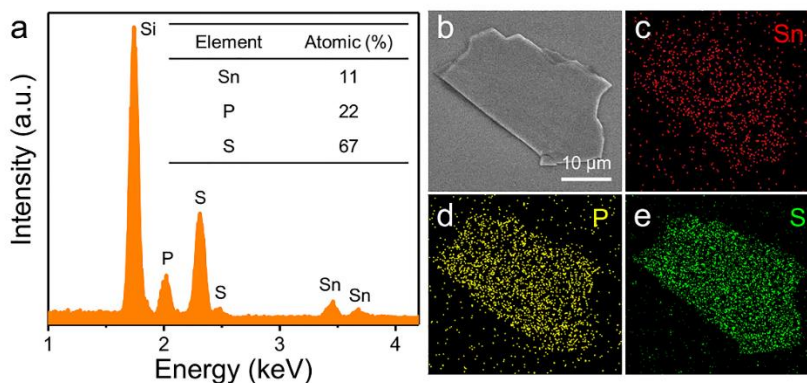


Figure S2 (a) EDS results of an exfoliated SnP₂S₆ flake. (b) SEM image of exfoliated SnP₂S₆ flake. (c-e) Sn, P and S element mapping of exfoliated SnP₂S₆ flake.

Address correspondence to Xiaozong Hu, huxz@zzu.edu.cn; Tianyou Zhai, zhaity@hust.edu.cn

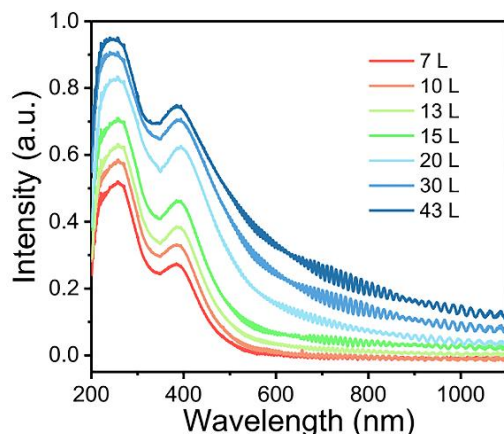


Figure S3 The absorption spectrum of SnP₂S₆ flakes with different thickness. It can be seen that the thicker flakes have the stronger absorption ability, which is consistent with the variation of Raman intensities of 2D SnP₂S₆.

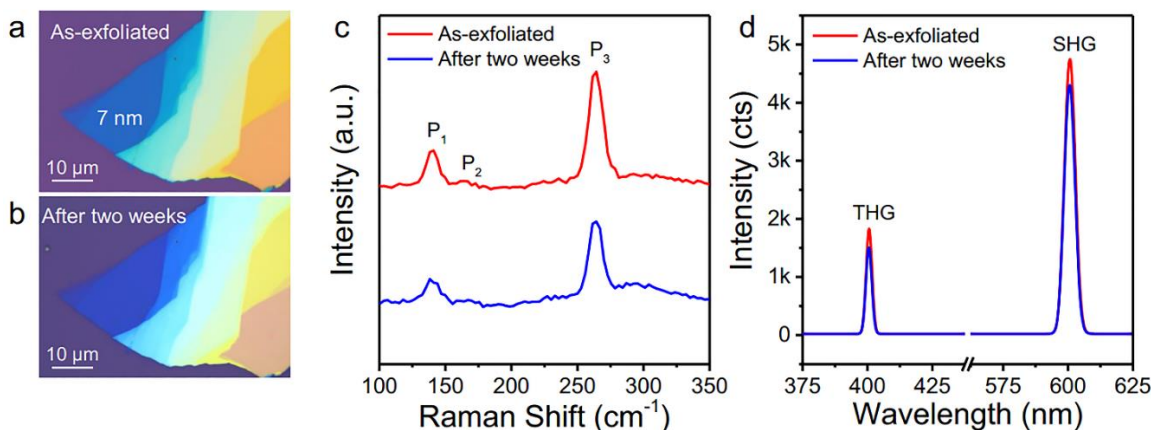


Figure S4 (a) The OM image of as-exfoliated SnP₂S₆ flakes. (b) The OM image of SnP₂S₆ flakes after being placed in air for two weeks. (c) Raman spectra and (d) NLO signal of 7 nm SnP₂S₆ flake at different times.

Calculation of Second-order nonlinear susceptibility

$$P_{2\omega} = \frac{8\pi^2 d^2}{\varepsilon_0 c \lambda^2 A} \cdot \frac{[\chi^{(2)}]^2}{n_{\omega}^2 n_{2\omega}} \cdot P_{\omega}^2 \quad (S1)$$

Where P_{ω} and $P_{2\omega}$ are excitation laser power and SHG power, respectively; $\chi^{(2)}$ is the second-order susceptibility; ε_0 and c are dielectric constant and the speed of light in vacuum, respectively; A is the area of the incident laser spot; d is the thickness of the sample to be measured; n_{ω} and $n_{2\omega}$ are the refractive index of SnP₂S₆ under excitation wavelength and SHG wavelength, respectively. Due to the SHG power cannot be measured directly, we will estimate the second-order susceptibility $\chi_{\text{SnP}_2\text{S}_6}^{(2)}$ of SnP₂S₆ by comparing with monolayer MoS₂ in the same test conditions (like same excitation power, wavelength, environment, etc.) [1, 2]. And the second-order susceptibility $\chi_{\text{MoS}_2}^{(2)}$ of monolayer MoS₂ has been measured previously. According to formula (S1), we can deduce the following formula

$$\frac{\chi_{\text{SnP}_2\text{S}_6}^{(2)}}{\chi_{\text{MoS}_2}^{(2)}} = \sqrt{\frac{P_{2\omega-\text{SnP}_2\text{S}_6}}{P_{2\omega-\text{MoS}_2}}} \cdot \frac{d_{\text{MoS}_2}}{d_{\text{SnP}_2\text{S}_6}} \cdot \sqrt{\frac{n_{2\omega-\text{SnP}_2\text{S}_6} n_{\omega-\text{SnP}_2\text{S}_6}^2}{n_{2\omega-\text{MoS}_2} n_{\omega-\text{MoS}_2}^2}} \quad (S2)$$

The SHG power is proportional to SHG intensity, so we can obtain formula (S3)

$$\chi_{\text{SnP}_2\text{S}_6}^{(2)} = \sqrt{\frac{I_{2\omega-\text{SnP}_2\text{S}_6}}{I_{2\omega-\text{MoS}_2}}} \cdot \frac{d_{\text{MoS}_2}}{d_{\text{SnP}_2\text{S}_6}} \cdot \sqrt{\frac{n_{2\omega-\text{SnP}_2\text{S}_6} n_{\omega-\text{SnP}_2\text{S}_6}^2}{n_{2\omega-\text{MoS}_2} n_{\omega-\text{MoS}_2}^2}} \cdot \chi_{\text{MoS}_2}^{(2)} \quad (S3)$$

Fig. S5 shows the SHG signal of 8 nm SnP₂S₆ and monolayer MoS₂ (prepared by chemical vapor deposition) under the same test environment. The incident wavelength is 810 nm, and $n_{2\omega-\text{MoS}_2}=3.4$, $n_{\omega-\text{MoS}_2}=4.12$, $n_{2\omega-\text{SnP}_2\text{S}_6}=3.26$ and $n_{\omega-\text{SnP}_2\text{S}_6}=2.8$, respectively. According to previous report, the second-order susceptibility $\chi_{\text{MoS}_2}^{(2)}$ of monolayer MoS₂ is about 10^{-7} m V⁻¹ at 810 nm excitation wavelength [3]. Therefore, we can estimate the second-order susceptibility $\chi_{\text{SnP}_2\text{S}_6}^{(2)}$ is approach 4.06×10^{-9} m V⁻¹ for 8 nm SnP₂S₆ flake from formula (S3).

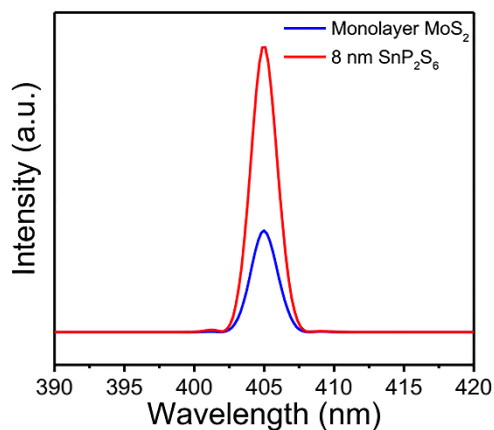


Figure S5 SHG signal for monolayer MoS₂ and 8 nm SnP₂S₆ flake under 810 nm excitation wavelength.

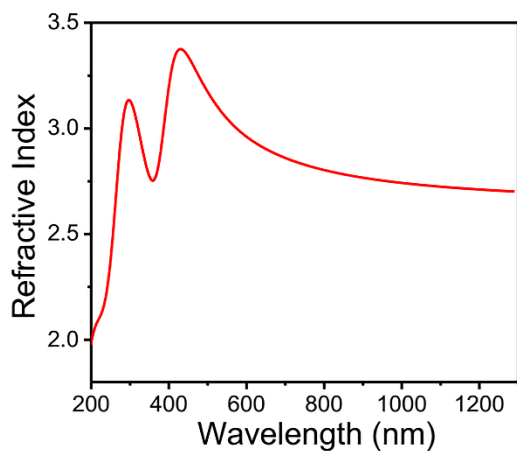


Figure S6 The refractive index of SnP₂S₆ crystal in the wavelength range of 200-1250 nm.

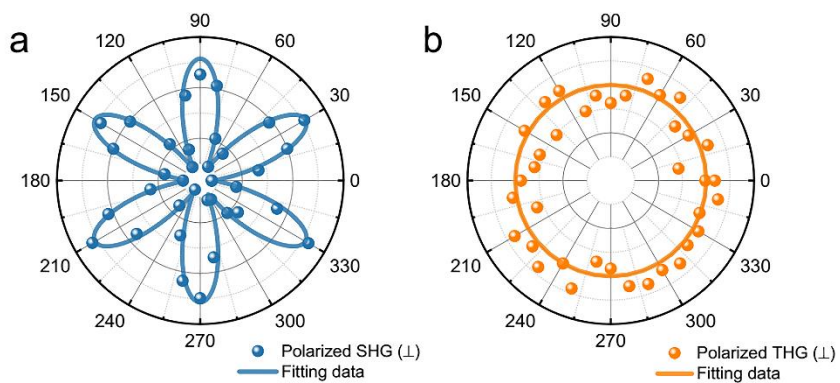


Figure S7 (a) and (b) are polarization-dependent SHG and THG intensity of SnP₂S₆ flake in perpendicular configuration.

References

- [1] Yang, D.; Hu, X.; Zhuang, M.; Ding, Y.; Zhou, S.; Li, A.; Yu, Y.; Li, H.; Luo, Z.; Gan, L., et al. Inversion symmetry broken 2D 3R-MoTe₂. *Adv. Funct. Mater.* **2018**, *28*, 1800785.
- [2] Shi, J.; Yu, P.; Liu, F.; He, P.; Wang, R.; Qin, L.; Zhou, J.; Li, X.; Zhou, J.; Sui, X., et al. 3R MoS₂ with broken inversion symmetry: a promising ultrathin nonlinear optical device. *Adv. Mater.* **2017**, *29*, 1701486.
- [3] Kumar N., Najmaei S., Cui Q., Ceballos F., Ajayan P. M., Lou J., Zhao H. Second harmonic microscopy of monolayer MoS₂. *Phys. Rev. B* **2013**, *87*, 161403.